Efficient Low-Complexity Antenna Selection Algorithms in Multi-User Massive MIMO Systems with Matched Filter Precoding

Zaid Abdullah, *Member, IEEE,* Charalampos C. Tsimenidis, *Senior Member, IEEE,* Gaojie Chen, *Senior Member, IEEE,* Martin Johnston, *Member, IEEE,* and Jonathon A. Chambers, *Fellow, IEEE*

***Abstract*—In this work, two efficient low complexity Antenna Selection (AS) algorithms are proposed for downlink Multi-User (MU) Massive Multiple-Input Multiple-Output (M-MIMO) systems with Matched Filter (MF) precoding. Both algorithms avoid vector multiplications during the iterative selection procedure to reduce complexity. Considering a system with N antennas at the Base Station (BS) serving K single-antenna users in the same time-frequency resources, the first algorithm divides the available antennas into K groups, with the kth group containing the N/K antennas that have the maximum channel norms for the kth user. Therefore, the Signal-to-Interference plus Noise Ratio (SINR) for the kth user can be maximized by selecting a subset of the antennas from only the kth group, thereby resulting in a search space reduction by a factor of K. The second algorithm is a semiblind interference rejection method that relies only on the signs of the interference terms, and at each iteration the antenna that rejects the maximum number of interference terms will be selected. The performance of our proposed methods is evaluated under perfect and imperfect Channel State Information (CSI) and compared with other low complexity AS schemes in terms of the achievable sum rate as well as the energy efficiency. In particular, when the Signal-to-Noise Ratio (SNR) is 10 dB, and for a system with 20 MHz of bandwidth, the proposed methods outperform the case where all the antennas are employed by 108.8 and 49.2 Mbps for the first and second proposed algorithms, respectively, given that the BS has perfect CSI knowledge and is equipped with 256 antennas, out of which 64 are selected to serve 8 single-antenna users.**

***Index Terms*—Massive MIMO, Antenna Selection, Multi-User, Complexity Reduction, Sum Rate, Energy Efficiency**

I. Introduction

Massive Multiple-Input Multiple-Output (M-MIMO) has been a hot topic of research in wireless communications in recent years, and it refers to a system where tens to hundreds of antennas are placed at the Base Station (BS) to serve a much smaller number of users. Compared to conventional MIMO systems, M-MIMO shows a great improvement in capacity and reliability while reducing the radiated energy dramatically [1], since increasing the number of antennas will provide additional degrees of freedom, which in return can be utilized to enhance the energy consumption of such systems [2]. For downlink transmission, precoding techniques should be applied to map the $K \times 1$ symbol vector intended for the K single-antenna users into an $N \times 1$ data vector before being transmitted through the wireless channel, where N is the number of antennas at the BS, $N \gg K$. The two most common types of linear precoding are Matched Filter (MF) and Zero Forcing (ZF) [3]. However, in this paper we consider only MF precoding since ZF does not only require higher complexity for finding the pseudo inverse of the channel matrix, but also can suffer from serious performance limitations. For example, one of the main limitations of ZF is that when the number of users grows large for a fixed number of antennas at the BS, the ZF precoder suffers from a sum rate loss [4], since most of the power will be used to null the interference. Moreover, the ZF suffers from degraded performance when there are users located on the cell-edge, also known as the "near-far" problem. In addition, the ZF precoder is very sensitive to different types of distortions such as unmodeled interference [5], [6]. In contrast, MF precoding requires lower processing complexity and can accommodate more users than ZF.

Although increasing the number of antennas at the BS offers great advantages in terms of performance, it does come at the price of increased hardware complexity, cost, and power consumption. Employing all the antennas means that each antenna should be connected to a separate Radio Frequency (RF) chain, and each RF chain consists of a mixer, analogue to digital converter, and amplifier. Therefore, and unlike the antenna elements, RF chains are expensive. Moreover, RF chains are considered as highly power demanding elements, and they consume 50%-80% of the total transceiving power [7]. One way to reduce the hardware complexity, cost, and power consumption while keeping the advantages of a M-MIMO system, is by applying Antenna Selection (AS) schemes [8]. Therefore, designing an efficient low complexity AS algorithm is an important topic in M-MIMO systems.

There has been a considerable amount of work on AS with both conventional and M-MIMO systems, for example, in [4], it was found that not all antennas contribute equally in M-MIMO systems, and AS can reduce the complexity and cost of M-MIMO without large degradation in the performance; while the authors in [9] designed an AS scheme to reject

This work was supported by EPSRC grant number EP/R006377/1 ("M3NETs").

Z. Abdullah, G. Chen and J. A. Chambers are with the Digital Communicatoins and Intelligent Sensing Group, School of Engineering, University of Leicester, LE1 7RH, UK. Emails: {zaid.abdullah; gaojie.chen; jonathon.chambers}@leicester.ac.uk.

C. Tsimenidis, and M. Johnston are with the Intelligent Sensing and Communications Group, Newcastle University, Newcastle-upon-Tyne, UK. Emails: {charalampos.tsimenidis; martin.johnston}@ncl.ac.uk.

the co-channel interference for a single user uplink scenario. Moreover, the authors in [10] and [11] aimed to enhance the error performance through AS by exploiting the temporal correlation, and the constructive interference, respectively. Although the proposed algorithm in [11] has low complexity, it works efficiently only for low modulation Phase Shift Keying (PSK) signalling, and it is data dependent, which means that extremely fast RF switching is required. Furthermore, the authors in [12] and [13] addressed the design of AS algorithms to maximize the Energy Efficiency (EE) of point-to-point M-MIMO systems. The authors in [14] proposed a novel iterative AS method for an uplink point-to-point M-MIMO system with a Maximum Ratio Combining (MRC) receiver, under spatially correlated channels. Their work focused on minimizing the Mean Square Error (MSE) of the received signal to improve the error rate performance for a single user scenario. The authors in [15] proposed a Rectangular Maximum-Volume (RMV) theory based AS technique, for downlink M-MIMO systems. However, their work focused on maximizing the sum rate capacity, which can be obtained via high complexity dirty paper coding. Moreover, the authors in [16] and [17] designed an AS algorithm with quartic complexity in point-to-point M-MIMO systems, while the authors in [18] studied the trade-off between energy and spectral efficiencies under random AS in Multi-User (MU) M-MIMO downlink systems. Moreover, in [19], the authors proposed an AS scheme under interference alignment, where the interference is forced to zero through transmitter-receiver beamforming. The authors in [20] proposed an AS method for power minimization in MU downlink M-MIMO systems, under a predefined Quality of Service (QoS) requirement. In addition, the authors in [21] and [22] proposed a joint AS and user scheduling scheme with ZF precoding. Finally, the authors in [23] showed that when MF precoding is applied, removing certain antennas can improve the sum rate performance of the system, and they proposed a low complexity greedy AS algorithm for sum rate maximization in downlink M-MIMO systems.

In this paper, we design two novel AS algorithms for downlink MU M-MIMO systems for Signal-to-Interference plus Noise Ratio (SINR) maximization with low complexity. Our contributions in this paper, which to the best of our knowledge have not been considered in any previously published work, can be summarized as follows

1) We design a User-Centric AS (UCAS) algorithm with reduced search space, where the available antennas are divided into K groups, and each group corresponds to only one user, where the kth group contains the antennas that have the maximum channel norms for the kth user. Therefore, to maximize the SINR for the kth user at a given iteration, the proposed algorithm selects an antenna from only the kth group. This reduces the search space by a factor of K.
2) The second proposed algorithm, called Semiblind Interference Rejection AS (SIRAS), is designed to reject the highest number of interuser interference terms at any given iteration, based on the signs of only the interference terms.
3) Both algorithms avoid any vector multiplications during the iterative selection process by storing the multiplications of any two entries in the channel matrix before the iterative algorithms start. This results in dramatic complexity reduction in terms of number of floating-point operations (FLOPs) required for their implementations.
4) The performance of the proposed algorithms is evaluated in terms of the achievable sum rate, energy efficiency, as well as computational complexity, and compared with other low complexity AS algorithms. Our proposed methods demonstrate an improved performance-complexity trade-off.

The rest of this paper is organized as follows. In Section II, we introduce the system model and formulate the AS problem. In Section III, the proposed AS algorithms are introduced and explained in detail. In Section IV, different numerical results are presented along with their discussions. The complexities of the different AS algorithms used in this work are evaluated in Section V in terms of number of FLOPs required for their implementations. Finally, the conclusions are drawn in Section VI.

TABLE I
LIST OF NOTATIONS USED IN THIS WORK

Notation	Explanation
$\|\|\mathbf{a}\|\|$	The Frobenius norm of vector $\mathbf{a}$
$\mathbf{a}^*$	The element-wise conjugate of vector $\mathbf{a}$
$\mathbf{a}^T$	The transpose of vector $\mathbf{a}$
$\mathbf{a}^H$	The Hermitian transpose of vector $\mathbf{a}$
$\Re[a]$	The real part of complex number a
$\Im[a]$	The imaginary part of complex number a
$\mathbf{0}_{M\times N}$	The M by N zero matrix
$\boldsymbol{I}_N$	The N by N identity matrix
$\mathbf{a}_i$	The ith row of matrix $\mathbf{A}$
$\mathbf{a}_j^c$	The jth column of matrix $\mathbf{A}$
$a_{i,j}$	The ith element of the jth column of $\mathbf{A}$
$\|a\|$	The absolute value of a
$a!$	The factorial operator
$\binom{a}{b}=\frac{a!}{b!(a-b)!}$	The binomial coefficient

The list of notations used throughout this work alongside their explanations are shown in Table I. We next introduce the model for the MU M-MIMO system.

II. System Model and Problem Formulation

A. Channel, signal, and noise models

We consider a single cell MU M-MIMO system operating in the downlink scenario as depicted in Fig. 1. Time Division

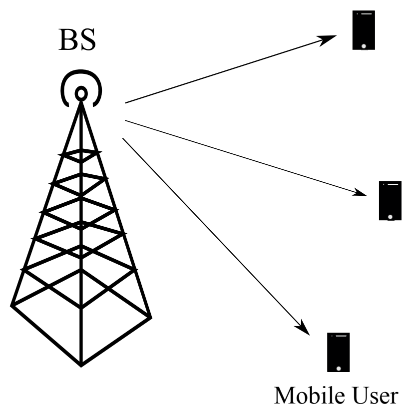

Fig. 1. MU M-MIMO downlink system.

Duplex (TDD) transmission is assumed, where the users send orthogonal pilots to the BS to obtain Channel State Information (CSI). Let $\mathbf{H} = [\mathbf{h}_1, \ldots, \mathbf{h}_K]^T \in \mathbb{C}^{K \times N}$ be the channel matrix, where $\mathbf{h}_k \in \mathbb{C}^{N \times 1}$ includes the channel coefficients between the BS and user k, with $h_{k,n} \sim \mathcal{CN}(0, \sigma_h^2)$, and let $\mathbf{w}_k \in \mathbb{C}^{N \times 1}$ denote the unit norm precoding vector for the kth user, and it can be given as

$$\mathbf{w}_k = \frac{\mathbf{h}_k^*}{\|\mathbf{h}_k\|}. \tag{1}$$

Assuming that the BS has perfect knowledge of $\mathbf{H}$, and MF precoding is applied, the transmitted signal vector from the BS to all users can be given as

$$\mathbf{s} = \sum_{k=1}^{K} \sqrt{p_k}\mathbf{w}_k x_k, \tag{2}$$

where $\boldsymbol{x} = [x_1, ..., x_K]^T$ is the vector of information symbols intended for the K users, with $E\{\boldsymbol{x}\boldsymbol{x}^H\} = \boldsymbol{I}_K$, p_k is the power allocated for the kth user, and it follows the constraint

$$\sum_{i=1}^{K} p_i = P_T, \tag{3}$$

where P_T is the total transmission power in Watts available at the BS for all users. Moreover, the received signal at the kth user can be given as

$$\begin{aligned} y_k &= \mathbf{h}_k^T \mathbf{s} + n_k \\ &= \sqrt{p_k}\mathbf{h}_k^T \mathbf{w}_k x_k + \sum_{\substack{i=1 \\ i \neq k}}^{K} \sqrt{p_i}\mathbf{h}_k^T \mathbf{w}_i x_i + n_k, \end{aligned} \tag{4}$$

where $n_k \sim \mathcal{CN}(0, \sigma_n^2)$ is the Additive White Gaussian Noise (AWGN) at the kth user.

B. SINR, achievable rates, and energy efficiency

In this work, we will use the sum rate and EE metrics to demonstrate the efficiency of the proposed AS algorithms. For systems with MF precoding, the SINR for the kth user can be expressed as [24]

$$\gamma_k = \frac{p_k \left|\mathbf{h}_k^T \mathbf{w}_k\right|^2}{\sum_{i=1,\ i \neq k}^{K} p_i \left|\mathbf{h}_k^T \mathbf{w}_i\right|^2 + \sigma_n^2}, \tag{5}$$

and the achievable rate for the same user is a function of the SINR, and it can be given as

$$R_k = \log_2(1 + \gamma_k), \tag{6}$$

while the total sum rate is the sum of achievable rates for all users, i.e.

$$R = \sum_{k=1}^{K} R_k. \tag{7}$$

Furthermore, the EE in bits/Joule can be defined as the total bandwidth, multiplied by the total sum rate over the total power consumed [13], i.e.

$$\text{EE} = \frac{B\ .\ R}{P_{total}}, \tag{8}$$

where B is the bandwidth, and P_{total} is the total power consumed at the transmitter and the receiver, and can be given as [25]

$$P_{total} = \frac{P_T}{\eta} + N_{RF}P_{tx} + KP_{rx}, \tag{9}$$

where η is the power amplifier efficiency, N_{RF} is the number of activated RF chains at the transmitter, while P_{tx} and P_{rx} are the circuit power consumption per RF chain at the transmitter and the receiver, respectively [25].

C. AS problem formulation

For a BS equipped with only N_s RF chains, AS schemes can be applied to optimize a certain cost function. In this work, we aim to select N_s out of the available N antennas at the BS to maximize the SINRs. This optimization problem can be formulated as follows

$$\underset{\boldsymbol{\Delta}}{\text{maximize}} \quad \sum_{k=1}^{K} \left(\frac{p_k \left|\mathbf{h}_k^T \boldsymbol{\Delta} \mathbf{w}_k\right|^2}{\sum_{\substack{i=1, \\ i \neq k}}^{K} p_i \left|\mathbf{h}_k^T \boldsymbol{\Delta} \mathbf{w}_i\right|^2 + \sigma_n^2} \right)$$

subject to

$$\Delta_{n,n} \in \{0, 1\}, \tag{10a}$$

$$\sum_{n=1}^{N} \Delta_{n,n} = N_s, \tag{10b}$$

where $\boldsymbol{\Delta}$ is a binary-valued $N \times N$ diagonal selection matrix. Providing the optimal solution requires an exhaustive search over $\binom{N}{N_s}$ different combinations of antenna subsets, therefore it becomes prohibitive for large values of N and N_s.

Accordingly, we propose in this paper two low-complexity, yet highly efficient, AS algorithms to solve the optimization problem in (10), and compare the performance of our proposed methods with the greedy selection algorithm proposed in [23, Algorithm 4]. It is noteworthy that the authors in [23] also considered a single-cell MU M-MIMO downlink system. However, their work focused on maximizing the sum rate through joint power allocation and AS as well as user scheduling, while in this work we focus only on the low-complexity design of AS schemes. It should be noted that throughout this work, we assume frequency-flat fading channels. Similar assumptions in M-MIMO systems with AS were made in [19], [26].

III. Proposed Antenna Selection Algorithms

Although MF is one of the most attractive forms of linear precoding, it suffers from inter-user interference, which causes a performance degradation. Both of the proposed algorithms depend on the channel cross-correlation matrix $\mathbf{U} = \mathbf{H}\mathbf{H}^H$, which can be expressed as

$$\mathbf{U} = \begin{pmatrix} \mathbf{h}_1^T\mathbf{h}_1^* & \mathbf{h}_1^T\mathbf{h}_2^* & \cdots & \cdots & \mathbf{h}_1^T\mathbf{h}_K^* \\ \mathbf{h}_2^T\mathbf{h}_1^* & \ddots & & & \vdots \\ \vdots & & \ddots & & \vdots \\ \vdots & & & \ddots & \mathbf{h}_{K-1}^T\mathbf{h}_K^* \\ \mathbf{h}_K^T\mathbf{h}_1^* & \cdots & \cdots & \cdots & \mathbf{h}_K^T\mathbf{h}_K^* \end{pmatrix}, \quad (11)$$

where the elements on the diagonal of (11) are related to the desired signal gain for each user, while the elements in the upper and lower triangular parts are directly related to the inter-user interference, since the interference from user j to user i is $\frac{|\mathbf{h}_i^T\mathbf{h}_j^*|^2}{\|\mathbf{h}_j\|^2}$, for $i, j = 1, 2, \ldots K$, and $i \neq j$. Each element in (11) is a summation of N multiplications between two complex numbers, i.e.

$$\mathbf{h}_i^T\mathbf{h}_j^* \;=\; h_{i,1}h_{j,1}^* + h_{i,2}h_{j,2}^* + \ldots.. + h_{i,N}h_{j,N}^*. \quad (12)$$

Both of the proposed algorithms aim to maintain low implementation complexity by avoiding vector multiplications during the iterative selection process as explained in the following subsections.

A. Proposed User-Centric Antenna Selection (UCAS) Algorithm

In this method, the antennas at the BS are divided into K groups based on their channel norms, where each group corresponds to one user. Moreover, each group should be allocated exactly N/K antennas, therefore, any group that reaches its maximum limit will not be considered in the allocation process for the remaining set of available antennas. The nth antenna at the BS will be allocated to the kth group, denoted as $\mathcal{G}_k$, only if it satisfies the following condition

$$h_{k,n} \in \mathcal{G}_k \iff |h_{k,n}| > |h_{i,n}|, \forall i \in \mathcal{K} \setminus k, \quad (13)$$

where $\mathcal{K}$ is a set containing the indices of groups with less than N/K antennas. For example, the 2nd antenna at the BS will be allocated to the 3rd group $\mathcal{G}_3$, if and only if $|h_{3,2}| > |h_{i,2}|, \forall i = 1, \ldots., K, i \neq 3$, and $\mathcal{G}_3$ has less than N/K antennas. The proposed grouping strategy is explained in detail in Algorithm 1.

At a given iteration, the UCAS algorithm aims to maximize the SINR for only the kth user, by selecting a single antenna from $\mathcal{G}_k$. For example, let $\underline{\mathbf{H}} = [\underline{\mathbf{h}_1}, \ldots, \underline{\mathbf{h}_K}]^T \in \mathbb{C}^{K \times t-1}$ be the channel matrix that corresponds to the $(t-1)$ selected antennas after as many iterations. Then, at the tth iteration, the antenna ζ will be selected as follows

$$\zeta = \arg\max_{n_s \in \mathcal{G}_k} \frac{\left| \underline{\mathbf{h}_k^T}\ \underline{\mathbf{h}_k^*} + h_{k,n_s}h_{k,n_s}^* \right|^2}{\sum_{\substack{i=1 \\ i \neq k}}^{K} \left| \underline{\mathbf{h}_k^T}\ \underline{\mathbf{h}_i^*} + h_{k,n_s}h_{i,n_s}^* \right|^2 + \sigma_n^2}. \quad (14)$$

Algorithm 1 Proposed grouping strategy for the UCAS method

```
Input K, N, and H,
Initialize
    G_k = 0_{N/K × 1}, ∀k ∈ {1, ..., K},
    t_k = 0, ∀k ∈ {1, ..., K}, (Number of antennas in each group),
    𝒦 = {1, ..., K}, (Set of indices of groups with less than N/K antennas),
for n = 1 → N
    k* = arg max_{k∈𝒦} |h_{k,n}|,
    t_{k*} = t_{k*} + 1,
    G_{k*}(t_{k*}) = n, (G_k(i) is the ith element of G_k),
    if t_{k*} = N/K
        𝒦 := 𝒦 \ k*,
    end if
end for
Output G_k, ∀k
```

Moreover, we aim to achieve further complexity reduction by avoiding any vector multiplications in the numerator and denominator of (14). Accordingly, we store the values of the N complex multiplications in (12), and for each element in (11), in a matrix $\mathbf{\Xi} \in \mathbb{C}^{K^2 \times N}$, which can be expressed as follows

$$\mathbf{\Xi} = \begin{pmatrix} \xi_{1,1} & \cdots & \cdots & \xi_{1,N} \\ \vdots & \ddots & & \vdots \\ \vdots & & \ddots & \vdots \\ \xi_{K,1} & \cdots & \cdots & \xi_{K,N} \\ \vdots & \ddots & & \vdots \\ \vdots & & \ddots & \vdots \\ \xi_{K^2,1} & \cdots & \cdots & \xi_{K^2,N} \end{pmatrix}, \quad (15)$$

where $\xi_{1,1} = h_{1,1}h_{1,1}^*$, $\xi_{1,N} = h_{1,N}h_{1,N}^*$, $\xi_{K,1} = h_{1,1}h_{K,1}^*$, $\xi_{K,N} = h_{1,N}h_{K,N}^*$, $\xi_{K^2,1} = h_{K,1}h_{K,1}^*$ and $\xi_{K^2,N} = h_{K,N}h_{K,N}^*$ (see Appendix A for details). Therefore, the SINR for the kth user depends mainly on rows $\{K(k-1)+1, K(k-1)+2, \ldots, Kk\}$ in $\mathbf{\Xi}$. Let $\mathcal{R}_k$ denote the set of row indices in $\mathbf{\Xi}$ that corresponds to user k, with $\mathcal{R}_{k_i}$ being the ith element of $\mathcal{R}_k$, for example, $\mathcal{R}_1 = \{1, 2, \ldots, K\}$, while $\mathcal{R}_{1_1} = 1$, and let $\boldsymbol{\omega} = [\omega_1, \omega_2, \ldots, \omega_{K^2}]^T$ be a vector initialized with zeros, and used to update the values of the signal and interference terms after each antenna is selected, since selecting any antenna from any group will result in adding a column from $\mathbf{\Xi}$ to $\boldsymbol{\omega}$. To clarify this, assume at iteration t, the antenna ζ was selected, the vector $\boldsymbol{\omega}$ will then be updated as follows

$$\boldsymbol{\omega}^{[t]} = \boldsymbol{\omega}^{[t-1]} + \boldsymbol{\xi}_{\zeta}^{c}, \quad (16)$$

and the selection of ζ can now be expressed as follows

$$\zeta = \arg\max_{n_s \in \mathcal{G}_k} \frac{\left| \omega_{\mathcal{R}_{k_k}}^{[t-1]} + \xi_{\mathcal{R}_{k_k}, n_s} \right|^2}{\sum_{\substack{i=1 \\ i \neq k}}^{K} \left| \omega_{\mathcal{R}_{k_i}}^{[t-1]} + \xi_{\mathcal{R}_{k_i}, n_s} \right|^2 + \sigma_n^2}. \quad (17)$$

Note that the selection process is now carried out without any vector multiplications. It should be noted that $\mathcal{G}_k$ is updated after the selection, by removing the index that corresponds to the selected antenna before the next iteration starts. In the next iteration, the selection will be carried out in a similar manner to maximize the SINR for the next user, i.e. the $(k+1)$th

Algorithm 2 Proposed UCAS algorithm

Input K, N, N_s, $\mathcal{G}_k(\forall k)$, $\mathcal{R}_k(\forall k)$, and $\mathbf{H}$,
Initialize
  $\boldsymbol{\omega} = \mathbf{0}_{K^2\times 1}$, $m = 0$, $\boldsymbol{\Xi} = \mathbf{0}_{K^2\times N}$,
for $i = 1 \rightarrow K$
  for $j = 1 \rightarrow K$
    $m = m + 1$,
    for $n = 1 \rightarrow N$
      $\xi_{m,n} = h_{i,n}h^*_{j,n}$,
    end for
  end for
end for
for $l = 1 \rightarrow N_s/K$
  for $k = 1 \rightarrow K$
    $\zeta = \arg\max_{n_s\in\mathcal{G}_k} \frac{\left|\omega_{\mathcal{R}_{k_k}} + \xi_{\mathcal{R}_{k_k},n_s}\right|^2}{\sum_{\substack{i=1\\i\neq k}}^{K}\left|\omega_{\mathcal{R}_{k_i}} + \xi_{\mathcal{R}_{k_i},n_s}\right|^2 + \sigma_n^2}$,
    $\boldsymbol{\omega} := \boldsymbol{\omega} + \boldsymbol{\xi}^c_{\zeta}$,
    $\mathcal{G}_k := \mathcal{G}_k \setminus \zeta$,
  end for
end for
Output $[\mathbf{H}^c_j]_{j\notin\mathcal{G}_{k,\forall k}}$

user. It is worth mentioning that exactly N_s/K antennas are selected from each group to ensure fairness between all users. The proposed UCAS scheme is explained in detail as shown in Algorithm 2.

B. Proposed Semiblind Interference Rejection Antenna Selection (SIRAS) Algorithm

The SIRAS algorithm aims to minimize the interuser interference by minimizing the terms in the upper and lower triangle parts of (11) relying only on the signs of the interference terms, hence the term semiblind. Furthermore, since $\mathbf{h}_i^T\mathbf{h}_j^* = (\mathbf{h}_j^T\mathbf{h}_i^*)^*$, it is sufficient to minimize the elements in the upper triangular part only, and that will lead to exactly the same minimization for the terms in the lower triangular part, and vice versa. The algorithm starts by storing the $M \times N$ complex multiplications in $\boldsymbol{\Phi}$, where $M = (K^2 - K)/2$ is the number of interference terms in the upper triangular part of (11), and it can be expressed as follows

$$\boldsymbol{\Phi} = \begin{pmatrix} \phi_{1,1} & \cdots & \cdots & \phi_{1,N} \\ \vdots & \ddots & & \vdots \\ \vdots & & \ddots & \vdots \\ \phi_{M,1} & \cdots & \cdots & \phi_{M,N} \end{pmatrix}. \tag{18}$$

Since the upper triangular part of (11) is considered in this work, the N elements in the first row of (18) are the values of the N complex number multiplications in the first interference term in (11), i.e. $\phi_{1,n} = h_{1,n}h^*_{2,n}$, while $\phi_{M,n} = h_{K-1,n}h^*_{K,n}$, for $n = 1, 2, ..., N$ (see Appendix A for details). The algorithm then selects its first antenna based on the maximum total channel norms

$$\zeta^{[0]} = \arg\max_{n\in 1:N} \|\mathbf{h}^c_n\|, \tag{19}$$

where $\zeta^{[0]}$ is the first selected antenna. After selecting the first antenna, a vector $\boldsymbol{\psi} \in \mathbb{C}^{M\times 1}$ will be initialized with the column in $\boldsymbol{\Phi}$ that corresponds to the selected antenna,

Algorithm 3 Proposed SIRAS algorithm

Input K, N, N_s, M, and $\mathbf{H}$,
Initialize:
  $\boldsymbol{\psi} = \mathbf{0}_{M\times 1}$, $\boldsymbol{\Phi} = \mathbf{0}_{M\times N}$, $m = 0$,
  $\mathcal{M} = \mathbf{0}_{1\times N}$, (set containing the indices of selected antennas)
  $\mathcal{A} = 1 \rightarrow N$, (set containing the indices of available antennas)
for $i = 1 \rightarrow K - 1$
  for $j = i + 1 \rightarrow K$
    $m = m + 1$,
    for $n = 1 \rightarrow N$
      $\phi_{m,n} = h_{i,n}h^*_{j,n}$,
    end for
  end for
end for
$\zeta^{[0]} = \arg\max_{n\in 1:N} \|\mathbf{h}^c_n\|$,
$\boldsymbol{\psi}^{[0]} = \boldsymbol{\phi}^c_{\zeta^{[0]}}$,
$\mathcal{A} := \mathcal{A} \setminus \zeta^{[0]}$,
$\mathcal{M}_{\zeta^{[0]}} = 1$,
for $t = 1 \rightarrow N_s$-1
  $\boldsymbol{\lambda} = \mathbf{0}_{1\times N-t}$, (vector containing the number of opposite signs between $\boldsymbol{\phi}$ and $\boldsymbol{\psi}$ for each available antenna),
  for $n = 1 \rightarrow N - t$
    for $m = 1 \rightarrow M$
      if sign($\Re[\phi_{m,\eta_n}]$) $\neq$ sign($\Re[\psi^{[t-1]}_m]$)
        $\lambda_n := \lambda_n + 1$,
      end if
      if sign($\Im[\phi_{m,\eta_n}]$) $\neq$ sign($\Im[\psi^{[t-1]}_m]$)
        $\lambda_n := \lambda_n + 1$,
      end if
    end for
  end for
  $\zeta = \arg\max \boldsymbol{\lambda}$,
  $\boldsymbol{\psi}^{[t]} = \boldsymbol{\psi}^{[t-1]} + \boldsymbol{\phi}^c_{\zeta}$,
  $\mathcal{A} := \mathcal{A} \setminus \zeta$,
  $\mathcal{M}_{\zeta} = 1$,
end for
Output: $[\mathbf{H}^c_j]_{j\notin\mathcal{A}}$

i.e. $\boldsymbol{\psi}^{[0]} = \boldsymbol{\phi}^c_{\zeta^{[0]}}$. Note that the M values in $\boldsymbol{\psi}$ are complex numbers, and they are directly related to the interference between the users at any given iteration, hence minimizing these values will result in minimizing the total interference and therefore higher SINRs. Moreover, selecting any antenna will result in adding a column from $\boldsymbol{\Phi}$ to $\boldsymbol{\psi}$. Assume that at iteration t, the antenna ζ was selected, then $\boldsymbol{\psi}$ will be updated as follows

$$\boldsymbol{\psi}^{[t]} = \boldsymbol{\psi}^{[t-1]} + \boldsymbol{\phi}^c_{\zeta}, \tag{20}$$

therefore, the goal is to select the antenna that corresponds to the column in $\boldsymbol{\Phi}$ which will minimize the M complex values in $\boldsymbol{\psi}$. In other words, at iteration t, the algorithm aims to select the antenna ζ from the set $\mathcal{S}$, where the nth antenna (denoted as λ_n) belongs to $\mathcal{S}$ if it satisfies the following condition

$$\lambda_n \in \mathcal{S} \iff \left\{\text{sign}(\Re[\phi_{m,n}]) \neq \text{sign}(\Re[\psi^{[t-1]}_m])\right\} \cap \left\{\text{sign}(\Im[\phi_{m,n}]) \neq \text{sign}(\Im[\psi^{[t-1]}_m])\right\}, \forall m, n \in \mathcal{A}, \tag{21}$$

where $\mathcal{A}$ is a set containing the indices of available antennas at a given iteration. However, it is not guaranteed to find an antenna that satisfies the condition in (21), therefore, we relax this condition and select the antenna that has the highest number of opposite signs between $\boldsymbol{\Phi}$ and $\boldsymbol{\psi}$. In the next iteration, the vector $\boldsymbol{\psi}$ will be updated according to (20), and the same procedure will be repeated again until maximum number of selected antennas is reached. The proposed method is described in detail in Algorithm 3.

IV. Numerical Results and Discussion

We apply Monte Carlo simulations to evaluate the spectral and energy efficiency performances of our proposed AS techniques for a wide range of Signal-to-Noise Ratios (SNRs). Furthermore, we compare our proposed algorithms with two low complexity AS methods. The first method is the Maximum SNR (MS) selection, where the N_s antennas with the highest channel gains are activated to serve the users in the cell. While the second technique is the low complexity greedy method proposed in [23, Algorithm 4]. However, it is worth mentioning that the work in [23] considers joint power allocation and AS, while here we focus only on the AS part.

Before discussing the results, we need to introduce the different parameters used in this work. First, we define the SNR per user as

$$\mathrm{SNR} = \frac{\sigma_h^2}{\sigma_n^2}\frac{P_T}{K}, \tag{22}$$

where the channel variance σ_h^2 can be found by using the path loss formula for a general urban channel model, which can be expressed as follows [27]

$$\mathrm{PL}\ (\mathrm{dB}) = 10\log_{10} d^{\alpha} + \beta, \tag{23}$$

where d is the distance between the users and the BS, α is the path loss component, and β is the fixed-loss component. In our simulations, and unless stated otherwise, d was set to 100 meters, α was assumed to be 2 as in [28], and β = 10 dB, therefore, $\sigma_h^2 = 10^{-5}$, while the noise variance σ_n^2 was assumed to have a value of 10^{-6}. Our assumption for equal distances between users and the BS is based on the fact that different distances from the BS for different users can be tackled through power allocation techniques based on large scale fading [29]. In addition, the bandwidth B was set to 20 MHz, the efficiency of the power amplifier η was 0.35, while the receive and transmit circuit power consumption per RF chain P_{rx} and P_{tx} were set to 62.5 mW and 48.2 mW, respectively [25]. Finally, the simulations were averaged over 10^4 different channels realizations for each SNR value.

A. Impact of AS on spectral and energy efficiencies

The advantage of designing efficient AS schemes when MF precoding is applied, in terms of spectral and energy efficiencies, can be seen in Figs. 2 and 3, respectively. Both of the proposed algorithms achieve higher rates with better EE than the full system case, where all the antennas are employed, i.e. when $N_s = N$. Furthermore, in terms of sum rate performance, increasing the SNR results in decreasing the number of antennas required to match the achievable rate where all antennas are activated. The reason behind this is that as the SNR increases, the effect of the noise becomes negligible, and the main factor that degrades the performance is the inter-user interference, and our proposed algorithms select the antennas that highly minimize the inter-user interference. In other words, although selecting a subset of the available antennas will reduce the signal gain, the resultant SINR will be higher, hence higher rates are achieved. Moreover, in terms of EE, applying AS techniques can dramatically improve the system performance as can be seen in Fig. 3. For example, when the number of selected antennas is 64, the UCAS and SIRAS algorithms outperform the full system case by 190.8 and 184 Mbits/Joule, respectively.

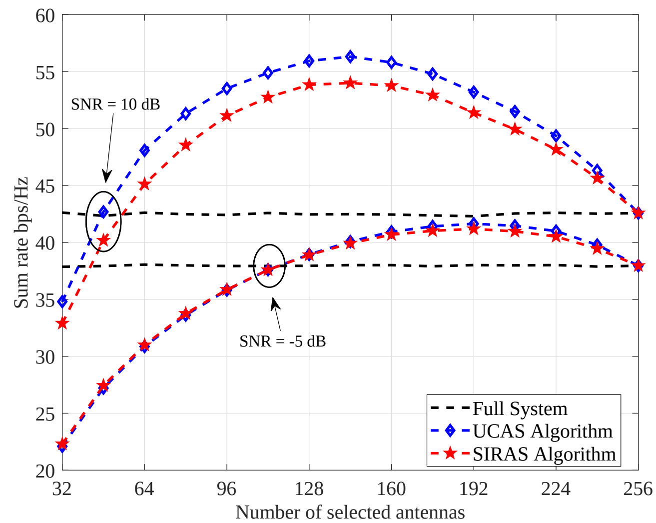

Fig. 2. Sum rate vs number of selected antennas for the proposed AS schemes when $N = 256$ and $K = 8$.

B. Achievable rates with fixed number of selected antennas

In this subsection, we show the performance of the proposed algorithms in terms of the achievable rates, and compare our results with MS and greedy selection techniques for a wide range of SNR values.

Fig. 4 shows the total sum rate when the BS is equipped with 128 antennas, out of which 32 are selected, for different AS schemes. The proposed algorithms outperform significantly both greedy and MS methods. Moreover, UCAS slightly outperforms the SIRAS algorithm when the SNR is less than 10 dB, while they both show the same performance for higher SNR values. For this scenario, employing all the available antennas at the BS achieves higher rates than our proposed algorithms when the number of selected antennas is 32.

Fig. 5 shows the total sum rate when 256 antennas are placed at the BS, and 64 antennas are selected by the proposed algorithms. The proposed methods not only outperform the greedy and MS techniques, but also the case where all the antennas are activated for SNR values higher than 0.5 dB and 3.5 dB for the UCAS and SIRAS algorithms, respectively.

From Fig. 5, the UCAS algorithm outperforms the full system, greedy, and MS selection methods at 10 dB SNR by 5.44, 10.12, and 19.64 bps/Hz, respectively, which correspond to a significant 108.8, 202.4, and 392.8 Mbps for a system with 20 MHz of bandwidth, while the SIRAS method shows an improvement of 2.46, 7.14, and 16.66 bps/Hz compared to the full system, greedy, and MS selection methods, respectively,

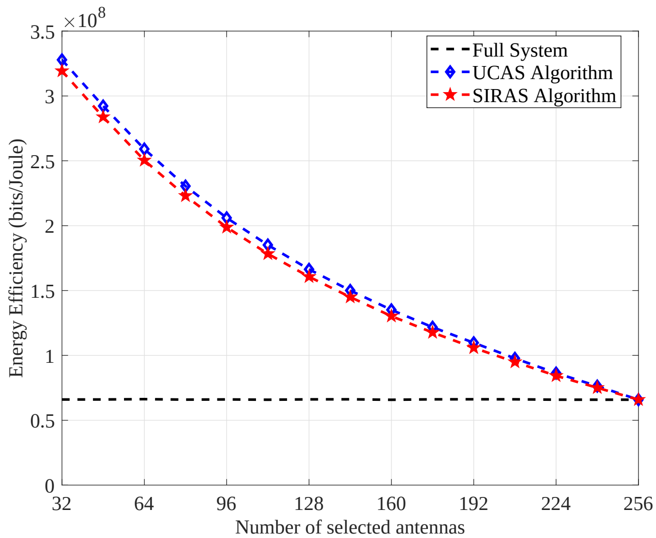

Fig. 3. Energy Efficiency vs number of selected antennas for the proposed AS schemes when $N = 256$, $K = 8$, $\sigma_n^2 = 10^{-9}$, and SNR = 10 dB.

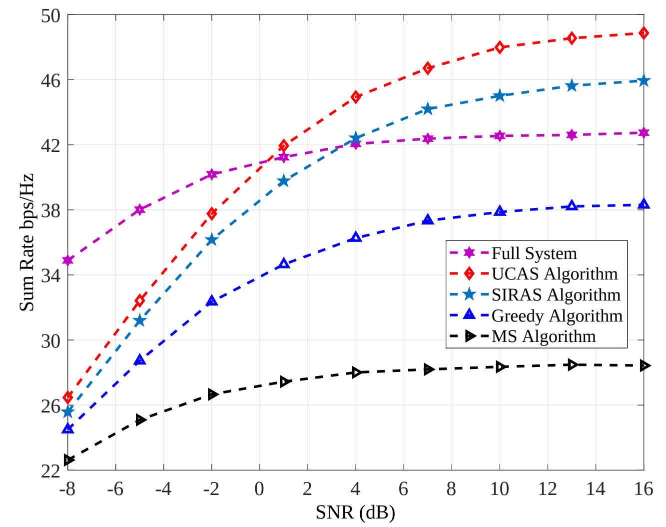

Fig. 5. Sum rate vs SNR (dB) for different AS schemes when $N = 256$, $N_s = 64$, and $K = 8$.

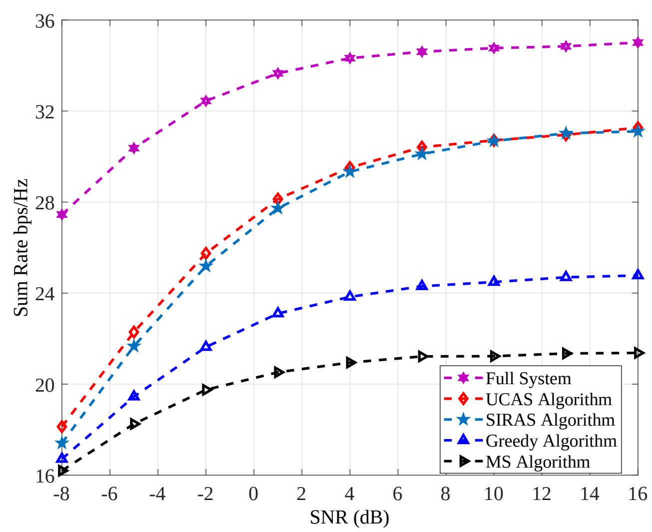

Fig. 4. Sum rate vs SNR (dB) for different AS schemes when $N = 128$, $N_s = 32$, and $K = 8$.

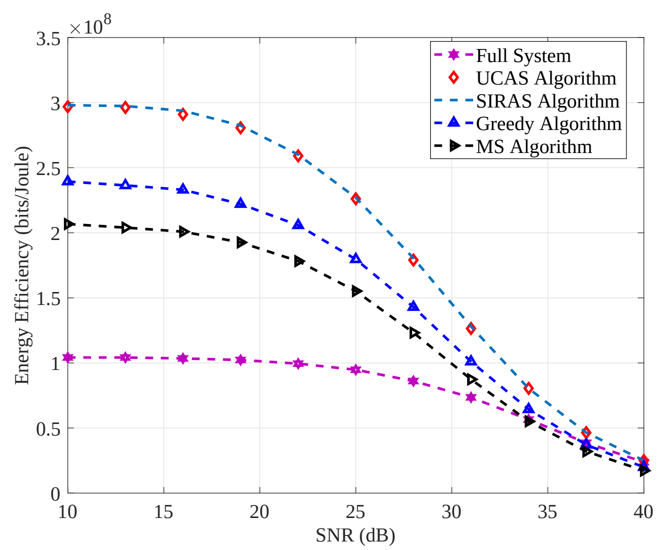

Fig. 6. EE vs SNR (dB) for different AS schemes when $\sigma_n^2 = 10^{-9}$, $N = 128$, $N_s = 32$, and $K = 8$.

at the same SNR value. Although the UCAS algorithm shows better performance than the SIRAS method, the latter occupies less memory space than UCAS, since the SIRAS relies on $\mathbf{\Phi}$ which has dimensions of $M \times N$, with $M = (K^2 - K)/2$, compared to $\mathbf{\Xi}$ for the UCAS which has dimensions of $K^2 \times N$.

C. Energy Efficiency Performance

In this subsection, we show the EE performance for the different AS methods as well as the full system case. We assume 128 antennas are placed at the BS, out of which 32 are selected to serve 8 users in the cell.

As Fig. 6 shows, at moderate SNR values, the proposed methods outperform significantly all other schemes for both scenarios. Furthermore, activating all the antennas results in extremely poor EE performance, which validates the importance of AS for energy efficient systems. For example, the proposed methods outperform the greedy algorithm, MS selection, and the full system by 59 Mbits/Joule, 92 Mbits/Joule, and 194 Mbits/Joule, respectively, at SNR of 10 dB.

D. Achievable rates with imperfect channel state information

In practical scenarios, the complex channel matrix $\mathbf{H}$ is estimated at the BS through pilot signals sent by the users, and channel estimation errors arise in any practical system. Different techniques have been designed to obtain the CSI in both conventional and M-MIMO systems [30]–[32]. In general, increasing the number of pilot signals leads to a better

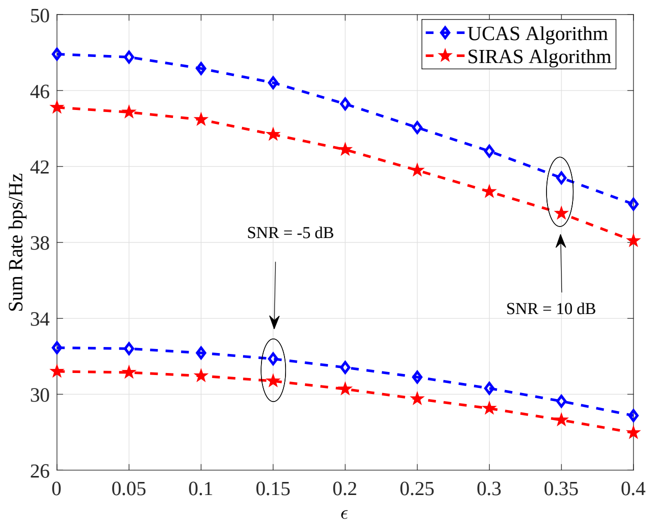

Fig. 7. Sum rate vs ϵ for the proposed AS schemes when $N = 256$, $N_s = 64$, and $K = 8$

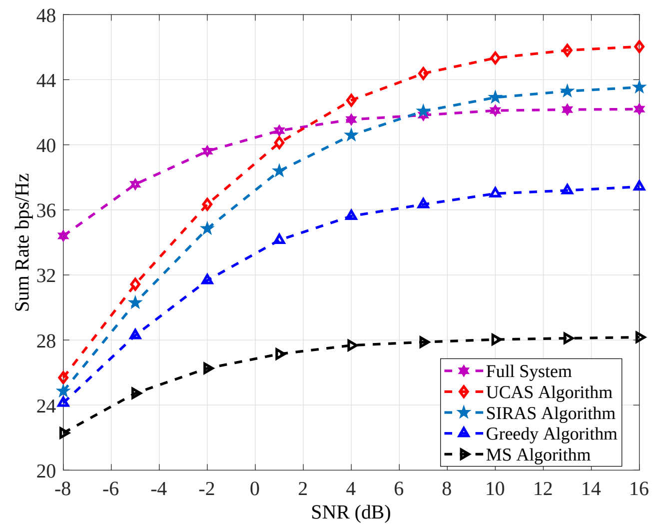

Fig. 8. Sum rate vs SNR (dB) for different AS schemes when $N = 256$, $N_s = 64$, $K = 8$ and $\epsilon = 0.2$.

estimation accuracy, but that comes at the price of a reduced data transmission interval. However, for M-MIMO systems, it was shown that a minimum of K pilot signals per coherence interval are enough when the system is operating in a TDD mode [33]. In this subsection, we evaluate the performance of the proposed algorithms under imperfect CSI. The estimated channel matrix $\widehat{\mathbf{H}}$ can be given as [34], [35]

$$\widehat{\mathbf{H}} = \mathbf{H} + \epsilon \boldsymbol{E}, \tag{24}$$

where $\epsilon\boldsymbol{E}$ represents the channel estimation error term, and is uncorrelated with $\mathbf{H}$. The entries of $\boldsymbol{E}$ are independent and identically distributed random variables with zero mean and variance of σ_h^2. Furthermore, ϵ controls the estimation accuracy, and $\epsilon = 0$ means the BS has a perfect CSI.

Fig. 7 demonstrates the achievable rates of the proposed methods for different levels of channel estimation error. The achievable rates are effected by the channel estimation accuracy for both methods. In addition, at higher SNR, the proposed algorithms become more sensitive under imperfect CSI. The reason behind this is that as the SNR increases, the noise effect becomes negligible, and the presence of CSI errors leads to the selection of sub-optimal antennas. For example, when the SNR $= -5$ dB, the UCAS and SIRAS algorithms suffer a 3.57 and 3.23 bps/Hz rate loss when $\epsilon = 0.4$ compared to the perfect CSI case, respectively; while the achievable rates for the same algorithms degrade by 7.92 and 7.11 bps/Hz, respectively, when $\epsilon = 0.4$, at SNR of 10 dB compared to the perfect CSI case.

Fig. 8 demonstrates the performance of different AS schemes for a wide range of SNR values when ϵ is 0.2. The UCAS and SIRAS algorithms outperform the full system case at 2 dB and 7 dB, respectively, compared to 0 dB and 4 dB for perfect CSI. Furthermore, at SNR $= 10$ dB, the UCAS algorithm outperforms the greedy method and MS selection by 8.34 bps/Hz and 17.34 bps/Hz, respectively; while the SIRAS method achieves 5.91 bps/Hz and 14.91 bps/Hz higher rates than the greedy method and MS selection, respectively, at the same SNR value.

E. Performance of the proposed methods with multiple random initializations

The performance of both of the proposed methods can be further enhanced by adopting multiple random initializations of users and antennas, for UCAS and SIRAS schemes, respectively. More specifically, for the UCAS method, after obtaining Ξ and grouping the antennas into K groups, the users were ordered from 1 to K, where for each of the N_s/K rounds of selection, one antenna was selected to maximize the SINR for the 1st user, followed by selecting one antenna to maximize the SINR for the 2nd user, and so forth until the Kth user. However, adopting multiple random initialization orders of the K users can further improve the performance by obtaining multiple sets of selected antennas, and then choose the set that achieves the highest SINR. Similarly, and for the SIRAS scheme, multiple random antennas can be chosen as the first selected antenna, and then perform the selection for the following $N_s - 1$ iterations to obtain different sets of selected antennas, and finally select the set that achieves the maximum total SINR.

As demonstrated in Fig. 9, both methods achieve a considerable gain when multiple random initial ordering of users and antennas are considered. Specifically, at a SNR of 10 dB, the UCAS scheme shows an improvement of 3.73 bps/Hz when 10 random initial orders ($L = 10$) of users are considered compared to the classical single ordering case ($L = 1$) shown in Algorithm 2. Moreover, the SIRAS scheme achieves a 4.03 bps/Hz gain when considering 10 random antennas as the first selected antenna ($L = 10$), compared to the case where the first selected antenna is only the one with the highest channel gain ($L = 1$). However, although these methods can provide

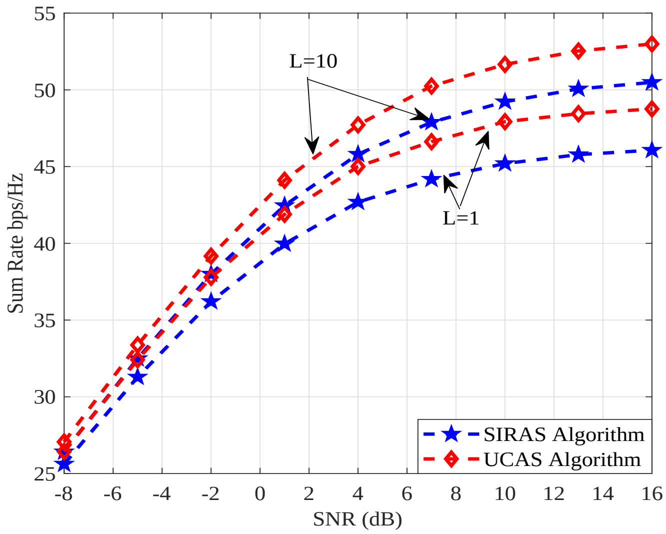

Fig. 9. Sum rate vs SNR (dB) for the proposed methods with different initial order when $N = 256$, $N_s = 64$, and $K = 8$.

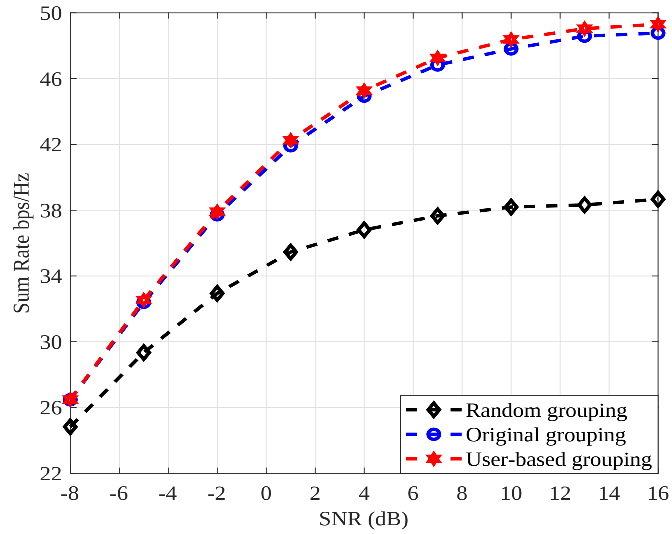

Fig. 10. Sum rate vs SNR (dB) for UCAS algorithm under different grouping schemes when $N = 256$, $N_s = 64$, and $K = 8$.

a considerable performance gain, they come at the price of increased complexity for their implementations as will be discussed in Section V.

F. Performance of UCAS algorithm under different grouping strategies

Throughout this work, grouping the antennas into K groups for the UCAS scheme was performed according to our proposed method in Algorithm 1. However, there are different methods to perform this part of the algorithm, and in this section, we will investigate the performance of two additional grouping strategies.

The first method is the random grouping strategy, where each group will randomly be assigned N/K antennas. A more efficient way of grouping is assigning the antenna that has the maximum channel gain with only the first user as the first assigned antenna for the first group. Followed by assigning the antenna that has the maximum channel gain with only the second user to the second group, and so forth until the Kth group. Moreover, the same procedure will be repeated until each group has N/K antennas assigned to it. We call the latter scheme as the user-based grouping.

As demonstrated in Fig. 10, the random grouping method shows an extremely poor performance compared to the other two grouping schemes. In contrast, the user-based grouping method shows a marginal sum rate improvement compared to the original grouping strategy given in Algorithm 1. However, the user-based grouping method requires higher complexity as will be demonstrated in Section V. Therefore, the original grouping method demonstrates a positive performance-complexity trade-off compared to the other two schemes.

G. Fairness measurement of the proposed AS schemes

To have more insight into the performance of the proposed AS schemes, we measure the equality among different users

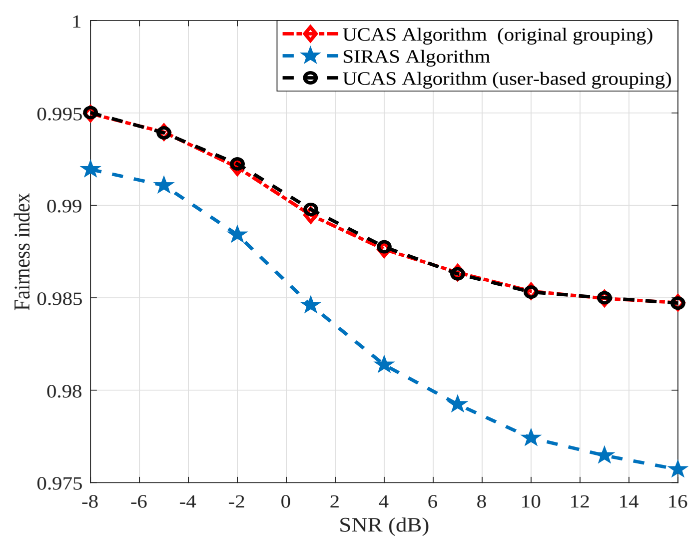

Fig. 11. Fairness index vs SNR (dB) when $N = 128$, $N_s = 32$, $K = 8$, and $L = 1$.

by applying Jain's equality formula, which can be defined as follows [36]

$$\text{Jain's fairness index} = \frac{\left(\sum_{k=1}^{K} R_k\right)^2}{K \sum_{k=1}^{K} R_k^2}. \quad (25)$$

As shown in Fig. 11, the proposed methods achieve near optimal fairness among the users, as the fairness index exceeds 97% for a wide range of SNR values. Moreover, the UCAS method, and regardless of the grouping strategy, can deliver higher fairness to users than the SIRAS scheme for the entire range of SNR values considered in this work.

TABLE II
NUMBER OF ADDITIONS AND MULTIPLICATIONS FOR DIFFERENT AS SCHEMES

Algorithm	Operator	Additions	Multiplications
MS	$\|\|\mathbf{h}_n^c\|\|, \forall n$	$N(2K-1)$	$N(2K+1)$
	Sorting	$N\log N$	$--$
	Total	$N(2K+\log N-1)$	$N(2K+1)$
Greedy	$\|\|\mathbf{h}_n^c\|\|, \forall n$	$N(2K-1)$	$N(2K+1)$
	Sorting	$N\log N$	$--$
	$\mathbf{w}_k, \forall k$	$\sum_{l=1}^{N_s} K(2l-1)$	$\sum_{l=1}^{N_s} K(4l+1)$
	$\gamma_k, \forall k$	$K\sum_{l=1}^{N_s}(4Kl-1)$	$K\sum_{l=1}^{N_s}(4Kl+5K+1)$
	R	$(2K-1)N_s$	$--$
	Total	$N(2K+\log N-1)-N_s+\sum_{l=1}^{N_s} l(4K^2+2K)$	$N(2K+1)+N_s(5K^2+2K)+\sum_{l=1}^{N_s} l(4K^2+4K)$
UCAS	$\boldsymbol{\Xi}$	$2K^2N$	$4K^2N$
	$\mathcal{G}_{k,\forall k}$	$2KN$	$3KN$
	$\zeta, \forall t\in\{1,...,N_s\}$	$\sum_{l=1}^{N_s/K}(\frac{N}{K}-l)4K^2$	$\sum_{l=1}^{N_s/K}(\frac{N}{K}-l)(4K^2+K)$
	$\boldsymbol{\omega}^{[t]}, \forall t\in\{1,...,N_s\}$	$2K^2N_s$	$--$
	Total	$K(2KN+2N+2KN_s)+\sum_{l=1}^{N_s/K}(\frac{N}{K}-l)4K^2$	$N(4K^2+3K)+\sum_{l=1}^{N_s/K}(\frac{N}{K}-l)(4K^2+K)$
SIRAS	$\boldsymbol{\Phi}$	$N(K^2-K)$	$2N(K^2-K)$
	$\|\|\mathbf{h}_n^c\|\|, \forall n$	$N(2K-1)$	$N(2K+1)$
	$\zeta^{[0]}$	N	$--$
	$\boldsymbol{\lambda}$	$\sum_{l=1}^{N_s-1} 2(N-l)(K^2-K)$	$--$
	$\zeta, \forall t\in\{1,...,N_s-1\}$	$\sum_{l=1}^{N_s-1}(N-l)$	$--$
	$\boldsymbol{\psi}^{[t]}, \forall t\in\{1,...,N_s-1\}$	$(N_s-1)(K^2-K)$	$--$
	Total	$N(K^2+K)+(N_s-1)(K^2-K)+\sum_{l=1}^{N_s-1}(N-l)(2K^2-2K+1)$	$N(2K^2+1)$

V. COMPLEXITY ANALYSIS

In TDD M-MIMO systems with AS, the BS is required for each coherence interval, to perform channel estimation and AS to enable efficient uplink and downlink data transmission. Therefore, the complexity analysis presented in this section is of great importance to evaluate the efficiency of the proposed AS schemes in practical scenarios, since higher complexity requires longer processing time, thus reducing the data transmission interval, and vice versa. It is worth highlighting that state-of-the-art Digital Signal Processors (DSPs), such as that found on the TCI6638K2K DSP board designed by Texas instruments for the next generation of wireless networks, can support up to 153.6 GigaFLOPs per second [37].

We follow the complexity analysis in [38], where the addition between two real numbers is equivalent to 1 FLOP, while their multiplication is equivalent to 4 additions. Moreover, we assume that comparing the signs of two real numbers is equivalent to 1 addition, while finding the square root of a real number and division between two real numbers are each equivalent to one real multiplication.

A. Complexity of MS scheme

The MS method has the lowest complexity, however that comes at the price of performance degradation. Finding the channel norms for the N antennas requires $N(10K+3)$ FLOPs, while sorting the antennas requires $N\log_{10} N$ FLOPs, therefore, the total complexity is

$$\mathcal{C}_{MS} = N(10K+\log_{10} N+3). \tag{26}$$

B. Complexity of greedy AS algorithm [23, Algorithm 4]

The greedy algorithm starts by finding the channel norms for the N antennas and sorting them, which requires $N(10K+\log_{10} N+3)$ FLOPs. The algorithm will then start its iterations, where at each iteration the sum rate in (7) will be evaluated. Finding the MF precoding weights for all the users requires $K\sum_{l=1}^{Ns}(18l+3)$ FLOPs, while evaluating the SINRs for all users requires $\sum_{l=1}^{N_s}(20K^2l+20K^2+3K)$ FLOPs. Finally, calculating the sum rate after obtaining the SINR values takes $(2K-1)N_s$ FLOPs, therefore, the total complexity of the greedy algorithm can be given as

$$\mathcal{C}_{greedy} = N(10K+\log_{10} N+3)+N_s(20K^2+8K-1) \\ +\sum_{l=1}^{Ns} l(20K^2+18K). \tag{27}$$

However, here we only consider an ideal case for the greedy algorithm by assuming that each selected antenna will boost

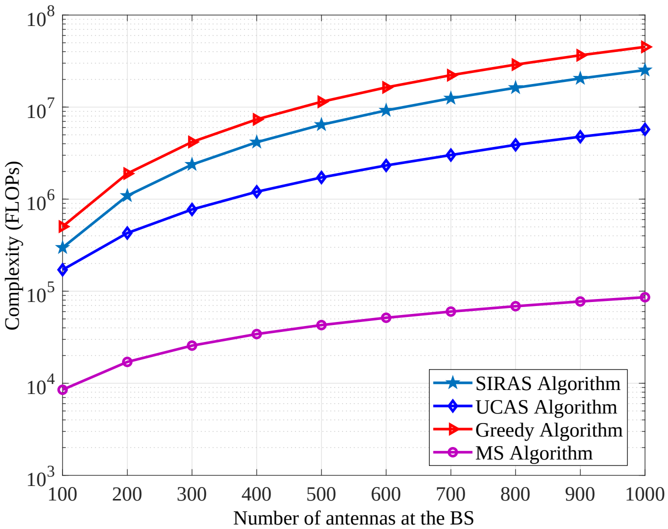

Fig. 12. Complexity in number of FLOPs vs number of antennas at the BS for different AS schemes when $N_s = N/4$, and $K = 8$.

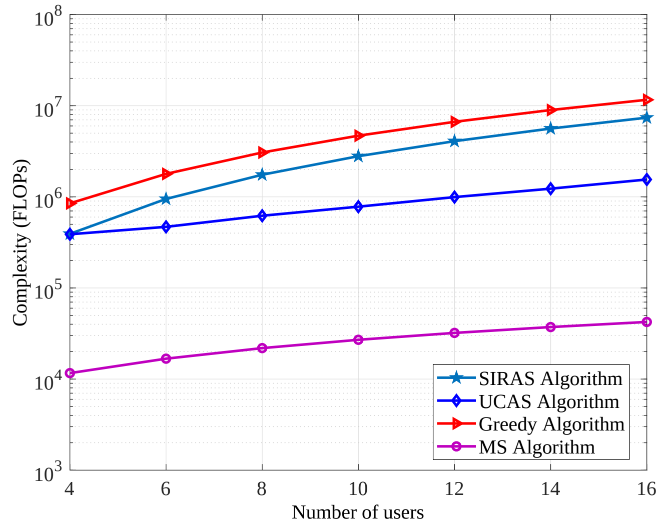

Fig. 13. Complexity in number of FLOPs vs number of users for different AS schemes when $N = 256$ and $N_s = N/4$.

the total sum rate, therefore, the actual complexity of the greedy algorithm is higher than that shown in this section, otherwise it would have shown the exact same sum rate performance as the MS scheme.

C. Complexity of UCAS algorithm with a single initial order of users ($L = 1$)

The UCAS algorithm starts by evaluating the matrix $\boldsymbol{\Xi}$ that has $K^2 \times N$ complex multiplications, which results in $18K^2N$ FLOPs. Then, the absolute channel values between the N antennas and K users are evaluated before being allocated to $\mathcal{G}_k, \forall k$ according to Algorithm 1, which results in $14KN$ FLOPs. The N_s/K iterations will then start to select K antennas at each iteration, which results in $\sum_{l=1}^{N_s/K}(20K+4)(N-Kl)$ FLOPs. Finally, the vector $\boldsymbol{\omega}$ is updated after selecting each antenna, which requires $2K^2N_s$ FLOPs. Therefore, the total number of FLOPs required by the UCAS algorithm can be given as

$$\mathcal{C}_{UCAS} = KN(18K+14) + 2K^2N_s + \sum_{l=1}^{N_s/K}(20K+4)(N-Kl). \tag{28}$$

D. Complexity of SIRAS algorithm with a single initial order of antennas ($L = 1$)

The SIRAS algorithm requires $9N(K^2-K)$ FLOPs to obtain $\boldsymbol{\Phi}$, after that, $N(10K+4)$ FLOPs are required to select the first antenna. The $N_s - 1$ iterations will then start, and at each iteration the vector $\boldsymbol{\lambda}$ is used to store the number of opposite signs, which takes $\sum_{l=1}^{N_s-1} 2(N-l)(K^2-K)$ FLOPs. Finding the $N_s - 1$ antennas from $\boldsymbol{\lambda}$ requires $\sum_{l=1}^{N_s-1}(N-l)$ FLOPs, and finally, updating the vector $\boldsymbol{\psi}$ results in $(N_s - 1)(K^2 - K)$ FLOPs. Therefore, the total complexity for the SIRAS algorithm can be given as

$$\mathcal{C}_{SIRAS} = N(9K^2+K+4) + (K^2-K)(N_s-1) + \sum_{l=1}^{N_s-1}(N-l)(2K^2-2K+1). \tag{29}$$

The numbers of additions and multiplications for the different AS schemes are shown for each operator in Table II[1]. It should be noted that in the aforementioned table, the number of additions also includes the comparison between the values or signs of two real numbers, while the number of multiplications includes the division as well as finding the square root of a real number.

Figs. 12 and 13 show the complexity for different AS schemes for different numbers of antennas N at the BS and different numbers of users K, respectively, with $N_s = N/4$. In both results, the MS algorithm has the lowest complexity, followed by the UCAS algorithm, then the SIRAS, while the greedy algorithm requires the highest complexity among the adopted schemes. As mentioned before, the actual complexity for the greedy algorithm is higher than that shown in this section, and here we only consider an ideal case.

To gain more insight on the efficiency of our proposed schemes in practical scenarios, assume that we have a BS equipped with 256 antennas, out of which 64 are selected to serve 8 single-antenna users. According to the analysis presented in this section, both of the proposed methods require less than 2×10^6 FLOPs, which corresponds to 13 μs of processing time using the aforementioned DSP board. Note that this is an impressive outcome for the proposed methods given that in the current Long-Term Evolution (LTE) standard, transmitting one symbol of data requires 71.4 μs [11].

[1]The number of additions and multiplications of UCAS and SIRAS methods shown in Table II are for the case where $L = 1$.

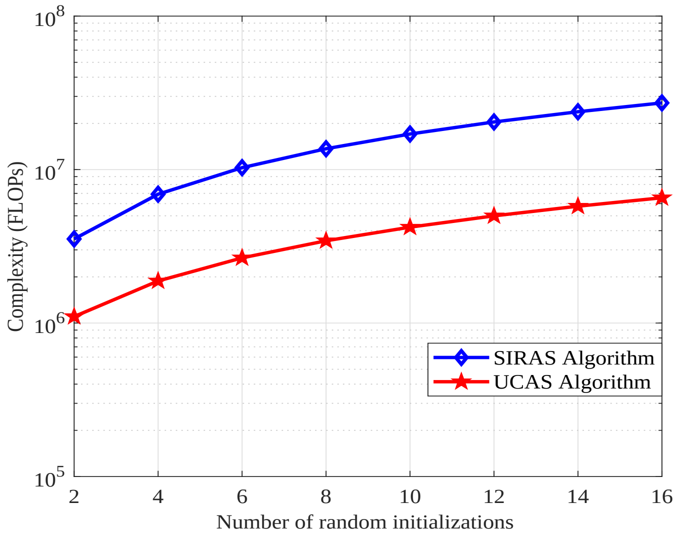

Fig. 14. Complexity in number of FLOPs vs number of random initial orders (L) for the proposed methods when N = 256, N_s = 64, and K = 8.

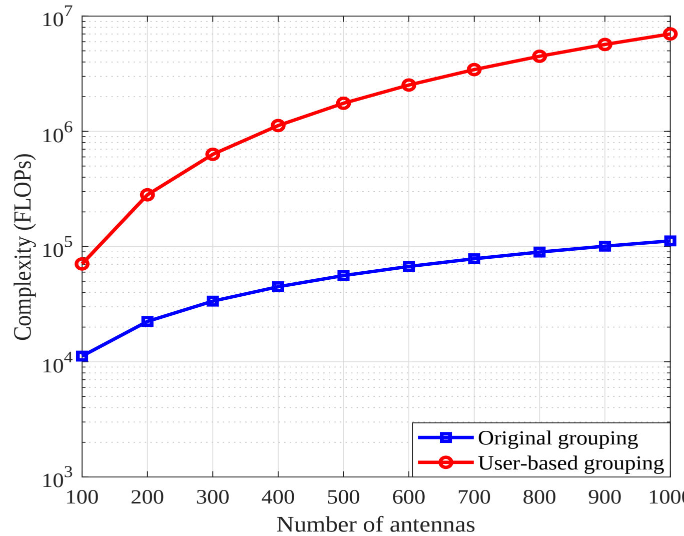

Fig. 15. Complexity in number of FLOPs vs number of antennas at the BS (N) for different grouping schemes when $K = 8$.

E. Complexity analysis of UCAS algorithm with multiple random ordering of users ($L > 1$)

The complexity required for obtaining L different candidate sets of selected antennas for the UCAS method, with $L > 1$, can be given as follows

$$\mathcal{C}_{UCAS}^{[L]} = L\mathcal{C}_{UCAS}^{[1]} - (L-1)(18K^2N + 14KN) + \mathcal{C}_{add}^{[L]}, \tag{30}$$

where $\mathcal{C}_{UCAS}^{[1]}$ is the complexity of UCAS method for a single initialization given in (28), and $C_{add}^{[L]}$ is the additional complexity required to evaluate the SINRs for the L candidates of different antenna subsets and selecting the one that has the maximum SINR as the final solution. For any number of random initializations $L > 1$, $\mathcal{C}_{add}^{[L]}$ can be given as follows

$$\mathcal{C}_{add}^{[L]} = L(20K^2N_s + 20K^2 + 18KN_s + 7K). \tag{31}$$

Finally, the second term in the right hand side of (30) is subtracted from the total complexity due to the fact that the matrix Ξ has to be evaluated only once, as well as grouping the antennas into the K groups according to Algorithm 1.

F. Complexity of SIRAS method with multiple random initializations of antennas ($L > 1$)

Similar to the UCAS method, the complexity of the SIRAS algorithm when $L > 1$ can be given as follows

$$\mathcal{C}_{SIRAS}^{[L]} = L\mathcal{C}_{SIRAS}^{[1]} - (L-1)(9NK^2 + NK + 4N) + \mathcal{C}_{add}^{[L]}, \tag{32}$$

where $\mathcal{C}_{SIRAS}^{[1]}$ is the complexity of the SIRAS method for a single initialization given in (29), $\mathcal{C}_{add}^{[L]}$ is the additional complexity to compute the SINRs of the L different antenna subsets given in (31), while the second term of the right hand side of (32) refers to the fact that the matrix Φ, sorting the antennas, and selecting the first antenna as the one with the maximum channel gain needs to be carried out only once.

As shown in Fig. 14, both methods suffer from increased complexity as the number of random initial orders (L) increases, with the SIRAS method requires higher complexity compared to the UCAS scheme.

G. Complexity of user-based grouping scheme

The complexity of the user-based grouping strategy requires $\sum_{l=1}^{N} 14(N-l+1)$ FLOPs to perform the grouping process, compared to $14KN$ FLOPs for the original approach given in Algorithm 1. As demonstrated in Fig. 15, the user-based grouping scheme requires much higher complexity than the original proposed grouping method, especially as the number of antennas at the BS increases.

VI. Conclusions

In this paper, two efficient low complexity AS algorithms were proposed for downlink MU M-MIMO systems with MF precoding. Dramatic complexity reduction was achieved by storing the multiplications between each two entries of the channel matrix to avoid any vector multiplications during the iterative selection process. The first algorithm divides the available antennas into K groups depending on their channel norms, where each group corresponds to one user only. This resulted in a search space reduction by a factor of K. The second algorithm was designed to reject the interuser interference relying only on the signs of the interference terms. The performance of the proposed methods under perfect and imperfect CSI was evaluated in terms of spectral and energy efficiencies. The proposed methods demonstrated great performance-complexity trade-off compared to other AS methods as well as to the case where all the antennas were employed.

Appendix A

The entries of matrices Ξ and Φ, for a system with 4 single-antenna users and 8 antennas at the BS, i.e. $K = 4$ and $N = 8$, can be defined as shown in (33) and (34), respectively.

Acknowledgements

The authors would like to express their gratitude to the Associate Editor, Dr. Vuk Marojevic, and to the anonymous reviewers for their constructive comments, which contributed to enhance the quality of this paper.

References

[1] F. Rusek, D. Persson, B. K. Lau, E. G. Larsson, T. L. Marzetta, O. Edfors, and F. Tufvesson, "Scaling up MIMO: Opportunities and challenges with very large arrays," *IEEE Signal Processing Mag.*, vol. 30, no. 1, pp. 40–60, Jan. 2013.

[2] M. Yao, M. Carrick, M. M. Sohul, V. Marojevic, C. D. Patterson, and J. H. Reed, "Semidefinite relaxation-based PAPR-aware precoding for massive MIMO-OFDM systems," *IEEE Trans. Veh. Technol.*, vol. 68, no. 3, pp. 2229–2243, Mar. 2018.

[3] H. Yang and T. L. Marzetta, "Performance of conjugate and zero-forcing beamforming in large-scale antenna systems," *IEEE J. Sel. Areas Commun.*, vol. 31, no. 2, pp. 172–179, Feb. 2013.

[4] X. Gao, O. Edfors, F. Tufvesson, and E. G. Larsson, "Massive MIMO in real propagation environments: Do all antennas contribute equally?" *IEEE Trans. Commun.*, vol. 63, no. 11, pp. 3917–3928, Nov. 2015.

[5] M. Sadek, A. Tarighat, and A. H. Sayed, "A leakage-based precoding scheme for downlink multi-user MIMO channels," *IEEE Trans. Wireless Commun.*, vol. 6, no. 5, pp. 1711–1721, May 2007.

[6] T. X. Tran and K. C. Teh, "Spectral and energy efficiency analysis for SLNR precoding in massive MIMO systems with imperfect CSI," *IEEE Trans. Wireless Commun.*, vol. 17, no. 6, pp. 4017–4027, Jun. 2018.

[7] L. M. Correia, D. Zeller, O. Blume, D. Ferling, Y. Jading, I. Gódor, G. Auer, and L. Van Der Perre, "Challenges and enabling technologies for energy aware mobile radio networks," *IEEE Commun. Mag.*, vol. 48, no. 11, pp. 66–72, Nov. 2010.

[8] N. B. Mehta, S. Kashyap, and A. F. Molisch, "Antenna selection in LTE: from motivation to specification," *IEEE Commun. Mag.*, vol. 50, no. 10, pp. 144–150, Oct. 2012.

[9] N.-D. Dao, J. Soler-Garrido, R. Cepeda, Y. Sun, and W. H. Chin, "Design and evaluation of antenna selection methods for interference rejection combining," *IEEE Trans. Wireless Commun.*, vol. 11, no. 8, pp. 2751–2759, Aug. 2012.

[10] S. Padmanabhan, R. G. Stephen, C. R. Murthy, and M. Coupechoux, "Training-based antenna selection for PER minimization: A POMDP approach," *IEEE Trans. Commun.*, vol. 63, no. 9, pp. 3247–3260, Sep. 2015.

[11] P. V. Amadori and C. Masouros, "Interference-driven antenna selection for massive multiuser MIMO," *IEEE Trans. Veh. Technol.*, vol. 65, no. 8, pp. 5944–5958, Aug. 2016.

[12] H. Li, L. Song, and M. Debbah, "Energy efficiency of large-scale multiple antenna systems with transmit antenna selection," *IEEE Trans. Commun.*, vol. 62, no. 2, pp. 638–647, Feb. 2014.

[13] C. Jiang and L. J. Cimini, "Antenna selection for energy-efficient MIMO transmission," *IEEE Wireless Commun. Letters*, vol. 1, no. 6, pp. 577–580, Dec. 2012.

[14] D. Mi, M. Dianati, S. Muhaidat, and Y. Chen, "A novel antenna selection scheme for spatially correlated massive MIMO uplinks with imperfect channel estimation," in *81st IEEE Veh. Tech. Conf. (VTC-Spring)*, Glasgow, UK, May, 2015, pp. 1–6.

[15] H. Tang and Z. Nie, "RMV antenna selection algorithm for massive MIMO," *IEEE Signal Process. Letters*, vol. 25, no. 2, pp. 239–242, Feb. 2018.

[16] M. Gkizeli and G. N. Karystinos, "Maximum-SNR antenna selection among a large number of transmit antennas," *IEEE J. Sel. Topics in Signal Process.*, vol. 8, no. 5, pp. 891–901, Oct. 2014.

[17] ——, "Maximum-SNR transmit antenna selection with two receive antennas is polynomially solvable," in *IEEE Int. Conf. Acoust., Speech, Signal Process. (ICASSP)*, Vancouver, Canada, May, 2013, pp. 4749–4753.

[18] Z. Liu, W. Du, and D. Sun, "Energy and spectral efficiency tradeoff for massive MIMO systems with transmit antenna selection," *IEEE Trans. Veh. Technol.*, vol. 66, no. 5, pp. 4453–4457, May 2017.

[19] M. Xie and T.-M. Lok, "Antenna selection in RF-chain-limited MIMO interference networks under interference alignment," *IEEE Trans. Veh. Technol.*, vol. 66, no. 5, pp. 3856–3870, May 2017.

[20] S. Qin, G. Li, G. Lv, G. Zhang, and H. Hui, "L1/2-regularization based antenna selection for RF-chain limited massive MIMO systems," in *84th IEEE Veh. Tech. Conf. (VTC-Fall)*, Montreal, Canada, Sep., 2016, pp. 1–5.

[21] M. Olyaee, M. Eslami, and J. Haghighat, "An energy-efficient joint antenna and user selection algorithm for multi-user massive MIMO downlink," *IET Communications*, vol. 12, no. 3, pp. 255–260, Nov. 2017.

[22] M. Benmimoune, E. Driouch, W. Ajib, and D. Massicotte, "Joint transmit antenna selection and user scheduling for massive MIMO systems," in *IEEE Wireless Commun. Net. Conf. (WCNC)*, New Orleans, LA, USA, Mar., 2015, pp. 381–386.

[23] R. Hamdi, E. Driouch, and W. Ajib, "Resource allocation in downlink large-scale MIMO systems," *IEEE Access*, vol. 4, pp. 8303–8316, Dec. 2016.

[24] C. Zhang, Y. Huang, Y. Jing, S. Jin, and L. Yang, "Sum-rate analysis for massive MIMO downlink with joint statistical beamforming and user scheduling," *IEEE Trans. Wireless Commun.*, vol. 16, no. 4, pp. 2181–2194, Apr. 2017.

[25] Y. Pei, T.-H. Pham, and Y.-C. Liang, "How many RF chains are optimal for large-scale MIMO systems when circuit power is considered?" in *IEEE Global Commun. Conf. (GLOBECOM)*, California, USA, Dec., 2012, pp. 3868–3873.

[26] Y. Gao, H. Vinck, and T. Kaiser, "Massive MIMO antenna selection: Switching architectures, capacity bounds, and optimal antenna selection algorithms," *IEEE Trans. Signal Process.*, vol. 66, no. 5, pp. 1346–1360, Mar. 2018.

[27] M. Hata, "Empirical formula for propagation loss in land mobile radio services," *IEEE Trans. Veh. Technol.*, vol. 29, no. 3, pp. 317–325, Aug. 1980.

[28] A. Yang, Z. He, C. Xing, Z. Fei, and J. Kuang, "The role of large-scale fading in uplink massive MIMO systems," *IEEE Trans. Veh. Technol.*, vol. 65, no. 1, pp. 477–483, Jan. 2016.

[29] O. Saatlou, M. O. Ahmad, and M. Swamy, "Spectral efficiency maximization of single cell massive multiuser MIMO systems via optimal power control with ZF receiver," in *28th IEEE Int. Symp. Personal, Indoor, and Mobile Radio Communications (PIMRC)*, Montreal, Canada, Oct., 2017, pp. 1–5.

[30] O. Bejarano, E. Magistretti, O. Gurewitz, and E. W. Knightly, "MUTE: sounding inhibition for MU-MIMO WLANs," in *11th Annu. IEEE Inter. Conf. Sens., Commun., Netw. (SECON)*, Singapore, Jul, 2014, pp. 135–143.

[31] X. Ma, Q. Gao, J. Wang, V. Marojevic, and J. H. Reed, "Dynamic sounding for multi-user MIMO in wireless LANs," *IEEE Trans. Consumer Electron.*, vol. 63, no. 2, pp. 135–144, May 2017.

[32] A. Khansefid and H. Minn, "On channel estimation for massive MIMO with pilot contamination," *IEEE Commun. Letters*, vol. 19, no. 9, pp. 1660–1663, Sep. 2015.

[33] T. L. Marzetta, E. G. Larsson, Y. Hong, and H. Q. Ngo, *Fundamentals of massive MIMO*. Cambridge Univ. Press, 2016.

[34] C. Wang, E. K. Au, R. D. Murch, W. H. Mow, R. S. Cheng, and V. Lau, "On the performance of the MIMO zero-forcing receiver in the presence of channel estimation error," *IEEE Trans. Wireless Commun.*, vol. 6, no. 3, Mar. 2007.

[35] B. Hassibi and B. M. Hochwald, "How much training is needed in multiple-antenna wireless links?" *IEEE Trans. Inf. Theory*, vol. 49, no. 4, pp. 951–963, Apr. 2003.

[36] M. A. Sedaghat and R. R. Müller, "On user pairing in uplink NOMA," *IEEE Trans. Wireless Commun.*, vol. 17, no. 5, pp. 3474–3486, May 2018.

[37] "CA-D8A4-RF4: Stand-alone baseband processing and RF card for eNodeB and UE in an LTE-A network," *Datasheet available at: www.ti.com*.

[38] R. J. Baxley and G. T. Zhou, "Comparing selected mapping and partial transmit sequence for PAR reduction," *IEEE Trans. Broadcasting*, vol. 53, no. 4, pp. 797–803, Dec. 2007.

$$
\begin{aligned}
\Xi &= \begin{bmatrix}
\xi_{1,1} & \xi_{1,2} & \xi_{1,3} & \xi_{1,4} & \xi_{1,5} & \xi_{1,6} & \xi_{1,7} & \xi_{1,8} \\
\xi_{2,1} & \xi_{2,2} & \xi_{2,3} & \xi_{2,4} & \xi_{2,5} & \xi_{2,6} & \xi_{2,7} & \xi_{2,8} \\
\xi_{3,1} & \xi_{3,2} & \xi_{3,3} & \xi_{3,4} & \xi_{3,5} & \xi_{3,6} & \xi_{3,7} & \xi_{3,8} \\
\xi_{4,1} & \xi_{4,2} & \xi_{4,3} & \xi_{4,4} & \xi_{4,5} & \xi_{4,6} & \xi_{4,7} & \xi_{4,8} \\
\xi_{5,1} & \xi_{5,2} & \xi_{5,3} & \xi_{5,4} & \xi_{5,5} & \xi_{5,6} & \xi_{5,7} & \xi_{5,8} \\
\xi_{6,1} & \xi_{6,2} & \xi_{6,3} & \xi_{6,4} & \xi_{6,5} & \xi_{6,6} & \xi_{6,7} & \xi_{6,8} \\
\xi_{7,1} & \xi_{7,2} & \xi_{7,3} & \xi_{7,4} & \xi_{7,5} & \xi_{7,6} & \xi_{7,7} & \xi_{7,8} \\
\xi_{8,1} & \xi_{8,2} & \xi_{8,3} & \xi_{8,4} & \xi_{8,5} & \xi_{8,6} & \xi_{8,7} & \xi_{8,8} \\
\xi_{9,1} & \xi_{9,2} & \xi_{9,3} & \xi_{9,4} & \xi_{9,5} & \xi_{9,6} & \xi_{9,7} & \xi_{9,8} \\
\xi_{10,1} & \xi_{10,2} & \xi_{10,3} & \xi_{10,4} & \xi_{10,5} & \xi_{10,6} & \xi_{10,7} & \xi_{10,8} \\
\xi_{11,1} & \xi_{11,2} & \xi_{11,3} & \xi_{11,4} & \xi_{11,5} & \xi_{11,6} & \xi_{11,7} & \xi_{11,8} \\
\xi_{12,1} & \xi_{12,2} & \xi_{12,3} & \xi_{12,4} & \xi_{12,5} & \xi_{12,6} & \xi_{12,7} & \xi_{12,8} \\
\xi_{13,1} & \xi_{13,2} & \xi_{13,3} & \xi_{13,4} & \xi_{13,5} & \xi_{13,6} & \xi_{13,7} & \xi_{13,8} \\
\xi_{14,1} & \xi_{14,2} & \xi_{14,3} & \xi_{14,4} & \xi_{14,5} & \xi_{14,6} & \xi_{14,7} & \xi_{14,8} \\
\xi_{15,1} & \xi_{15,2} & \xi_{15,3} & \xi_{15,4} & \xi_{15,5} & \xi_{15,6} & \xi_{15,7} & \xi_{15,8} \\
\xi_{16,1} & \xi_{16,2} & \xi_{16,3} & \xi_{16,4} & \xi_{16,5} & \xi_{16,6} & \xi_{16,7} & \xi_{16,8}
\end{bmatrix} \\
&= \begin{bmatrix}
h_{1,1}h^*_{1,1} & h_{1,2}h^*_{1,2} & h_{1,3}h^*_{1,3} & h_{1,4}h^*_{1,4} & h_{1,5}h^*_{1,5} & h_{1,6}h^*_{1,6} & h_{1,7}h^*_{1,7} & h_{1,8}h^*_{1,8} \\
h_{1,1}h^*_{2,1} & h_{1,2}h^*_{2,2} & h_{1,3}h^*_{2,3} & h_{1,4}h^*_{2,4} & h_{1,5}h^*_{2,5} & h_{1,6}h^*_{2,6} & h_{1,7}h^*_{2,7} & h_{1,8}h^*_{2,8} \\
h_{1,1}h^*_{3,1} & h_{1,2}h^*_{3,2} & h_{1,3}h^*_{3,3} & h_{1,4}h^*_{3,4} & h_{1,5}h^*_{3,5} & h_{1,6}h^*_{3,6} & h_{1,7}h^*_{3,7} & h_{1,8}h^*_{3,8} \\
h_{1,1}h^*_{4,1} & h_{1,2}h^*_{4,2} & h_{1,3}h^*_{4,3} & h_{1,4}h^*_{4,4} & h_{1,5}h^*_{4,5} & h_{1,6}h^*_{4,6} & h_{1,7}h^*_{4,7} & h_{1,8}h^*_{4,8} \\
h_{2,1}h^*_{1,1} & h_{2,2}h^*_{1,2} & h_{2,3}h^*_{1,3} & h_{2,4}h^*_{1,4} & h_{2,5}h^*_{1,5} & h_{2,6}h^*_{1,6} & h_{2,7}h^*_{1,7} & h_{2,8}h^*_{1,8} \\
h_{2,1}h^*_{2,1} & h_{2,2}h^*_{2,2} & h_{2,3}h^*_{2,3} & h_{2,4}h^*_{2,4} & h_{2,5}h^*_{2,5} & h_{2,6}h^*_{2,6} & h_{2,7}h^*_{2,7} & h_{2,8}h^*_{2,8} \\
h_{2,1}h^*_{3,1} & h_{2,2}h^*_{3,2} & h_{2,3}h^*_{3,3} & h_{2,4}h^*_{3,4} & h_{2,5}h^*_{3,5} & h_{2,6}h^*_{3,6} & h_{2,7}h^*_{3,7} & h_{2,8}h^*_{3,8} \\
h_{2,1}h^*_{4,1} & h_{2,2}h^*_{4,2} & h_{2,3}h^*_{4,3} & h_{2,4}h^*_{4,4} & h_{2,5}h^*_{4,5} & h_{2,6}h^*_{4,6} & h_{2,7}h^*_{4,7} & h_{2,8}h^*_{4,8} \\
h_{3,1}h^*_{1,1} & h_{3,2}h^*_{1,2} & h_{3,3}h^*_{1,3} & h_{3,4}h^*_{1,4} & h_{3,5}h^*_{1,5} & h_{3,6}h^*_{1,6} & h_{3,7}h^*_{1,7} & h_{3,8}h^*_{1,8} \\
h_{3,1}h^*_{2,1} & h_{3,2}h^*_{2,2} & h_{3,3}h^*_{2,3} & h_{3,4}h^*_{2,4} & h_{3,5}h^*_{2,5} & h_{3,6}h^*_{2,6} & h_{3,7}h^*_{2,7} & h_{3,8}h^*_{2,8} \\
h_{3,1}h^*_{3,1} & h_{3,2}h^*_{3,2} & h_{3,3}h^*_{3,3} & h_{3,4}h^*_{3,4} & h_{3,5}h^*_{3,5} & h_{3,6}h^*_{3,6} & h_{3,7}h^*_{3,7} & h_{3,8}h^*_{3,8} \\
h_{3,1}h^*_{4,1} & h_{3,2}h^*_{4,2} & h_{3,3}h^*_{4,3} & h_{3,4}h^*_{4,4} & h_{3,5}h^*_{4,5} & h_{3,6}h^*_{4,6} & h_{3,7}h^*_{4,7} & h_{3,8}h^*_{4,8} \\
h_{4,1}h^*_{1,1} & h_{4,2}h^*_{1,2} & h_{4,3}h^*_{1,3} & h_{4,4}h^*_{1,4} & h_{4,5}h^*_{1,5} & h_{4,6}h^*_{1,6} & h_{4,7}h^*_{1,7} & h_{4,8}h^*_{1,8} \\
h_{4,1}h^*_{2,1} & h_{4,2}h^*_{2,2} & h_{4,3}h^*_{2,3} & h_{4,4}h^*_{2,4} & h_{4,5}h^*_{2,5} & h_{4,6}h^*_{2,6} & h_{4,7}h^*_{2,7} & h_{4,8}h^*_{2,8} \\
h_{4,1}h^*_{3,1} & h_{4,2}h^*_{3,2} & h_{4,3}h^*_{3,3} & h_{4,4}h^*_{3,4} & h_{4,5}h^*_{3,5} & h_{4,6}h^*_{3,6} & h_{4,7}h^*_{3,7} & h_{4,8}h^*_{3,8} \\
h_{4,1}h^*_{4,1} & h_{4,2}h^*_{4,2} & h_{4,3}h^*_{4,3} & h_{4,4}h^*_{4,4} & h_{4,5}h^*_{4,5} & h_{4,6}h^*_{4,6} & h_{4,7}h^*_{4,7} & h_{4,8}h^*_{4,8}
\end{bmatrix},
\end{aligned}
\tag{33}
$$

$$
\begin{aligned}
\Phi &= \begin{bmatrix}
\phi_{1,1} & \phi_{1,2} & \phi_{1,3} & \phi_{1,4} & \phi_{1,5} & \phi_{1,6} & \phi_{1,7} & \phi_{1,8} \\
\phi_{2,1} & \phi_{2,2} & \phi_{2,3} & \phi_{2,4} & \phi_{2,5} & \phi_{2,6} & \phi_{2,7} & \phi_{2,8} \\
\phi_{3,1} & \phi_{3,2} & \phi_{3,3} & \phi_{3,4} & \phi_{3,5} & \phi_{3,6} & \phi_{3,7} & \phi_{3,8} \\
\phi_{4,1} & \phi_{4,2} & \phi_{4,3} & \phi_{4,4} & \phi_{4,5} & \phi_{4,6} & \phi_{4,7} & \phi_{4,8} \\
\phi_{5,1} & \phi_{5,2} & \phi_{5,3} & \phi_{5,4} & \phi_{5,5} & \phi_{5,6} & \phi_{5,7} & \phi_{5,8} \\
\phi_{6,1} & \phi_{6,2} & \phi_{6,3} & \phi_{6,4} & \phi_{6,5} & \phi_{6,6} & \phi_{6,7} & \phi_{6,8}
\end{bmatrix} \\
&= \begin{bmatrix}
h_{1,1}h^*_{2,1} & h_{1,2}h^*_{2,2} & h_{1,3}h^*_{2,3} & h_{1,4}h^*_{2,4} & h_{1,5}h^*_{2,5} & h_{1,6}h^*_{2,6} & h_{1,7}h^*_{2,7} & h_{1,8}h^*_{2,8} \\
h_{1,1}h^*_{3,1} & h_{1,2}h^*_{3,2} & h_{1,3}h^*_{3,3} & h_{1,4}h^*_{3,4} & h_{1,5}h^*_{3,5} & h_{1,6}h^*_{3,6} & h_{1,7}h^*_{3,7} & h_{1,8}h^*_{3,8} \\
h_{1,1}h^*_{4,1} & h_{1,2}h^*_{4,2} & h_{1,3}h^*_{4,3} & h_{1,4}h^*_{4,4} & h_{1,5}h^*_{4,5} & h_{1,6}h^*_{4,6} & h_{1,7}h^*_{4,7} & h_{1,8}h^*_{4,8} \\
h_{2,1}h^*_{3,1} & h_{2,2}h^*_{3,2} & h_{2,3}h^*_{3,3} & h_{2,4}h^*_{3,4} & h_{2,5}h^*_{3,5} & h_{2,6}h^*_{3,6} & h_{2,7}h^*_{3,7} & h_{2,8}h^*_{3,8} \\
h_{2,1}h^*_{4,1} & h_{2,2}h^*_{4,2} & h_{2,3}h^*_{4,3} & h_{2,4}h^*_{4,4} & h_{2,5}h^*_{4,5} & h_{2,6}h^*_{4,6} & h_{2,7}h^*_{4,7} & h_{2,8}h^*_{4,8} \\
h_{3,1}h^*_{4,1} & h_{3,2}h^*_{4,2} & h_{3,3}h^*_{4,3} & h_{3,4}h^*_{4,4} & h_{3,5}h^*_{4,5} & h_{3,6}h^*_{4,6} & h_{3,7}h^*_{4,7} & h_{3,8}h^*_{4,8}
\end{bmatrix}.
\end{aligned}
\tag{34}
$$

Zaid Abdullah (M'18) received the B.Sc. degree in electrical engineering (electronics and communications) from Mosul University, Mosul, Iraq, in 2012, and the M.Sc. and Ph.D. degrees in communications and signal processing from Newcastle University, U.K., in 2014 and 2019, respectively. He is currently a Postdoctoral Research Assistant with the Digital Communications and Intelligent Sensing Group, School of Engineering, University of Leicester, U.K. His main research interests include Massive MIMO systems, M2M, NOMA, physical layer security, and low complexity algorithms design.

Charalampos C. Tsimenidis (M'05, SM'12) received the M.Sc. (Hons.) and Ph.D. degrees in communications and signal processing from Newcastle University, in 1999 and 2002, respectively, where he is currently a Reader in digital communications with the School of Engineering. In the last 13 years, he has published over 180 conference and journal papers, has supervised successfully 3 M.Phil. and 45 Ph.D. students, and has made contributions in the area of receiver design to several European funded research projects. His main research interest includes adaptive array receivers for wireless communications, including demodulation algorithms and protocol design for doubly spread multipath channels.

Gaojie Chen (S'09-M'12-SM'18) received the B.Eng. and B.Ec. degrees in electrical information engineering and international economics and trade from Northwest University, China, in 2006, and the M.Sc. (Hons.) and Ph.D. degrees in electrical and electronic engineering from Loughborough University, Loughborough, U.K., in 2008 and 2012, respectively. From 2008 to 2009, he was a Software Engineering with DTmobile, Beijing, China, and from 2012 to 2013, he was a Research Associate with the School of Electronic, Electrical and Systems Engineering, Loughborough University. He was a Research Fellow with 5GIC, Faculty of Engineering and Physical Sciences, University of Surrey, U.K., from 2014 to 2015. Then he was a Research Associate with the Department of Engineering Science, University of Oxford, U.K., from 2015 to 2018. He is currently a Lecturer with the Department of Engineering, University of Leicester, U.K.
His current research interests include information theory, wireless communications, cooperative communications, cognitive radio, secrecy communication, and random geometric networks. He received the Exemplary Reviewer Certificate of the IEEE Wireless Communication Letters in 2018. He has served as an Editor for IET ELECTRONICS LETTERS (2018-present).

Martin Johnston (M'15) received his BSc (Hons) degree in Physics with Electronics from Birmingham University, UK, in 1999, his MSc degree in Electronic Engineering from Staffordshire University, UK, in 2001 and his PhD degree in 2006 from Newcastle University, UK. From 2006 - 2014 he worked as a Research Associate at the School of Engineering in Newcastle University and he is now employed as a Lecturer. His research interests include the design of advanced error-correcting schemes and low-complexity decoding algorithms, vehicle-to-vehicle communications and physical-layer security.

Jonathon A. Chambers (S'83–M'90–SM'98–F'11) received the Ph.D. and D.Sc. degrees in signal processing from the Imperial College of Science, Technology and Medicine (Imperial College London), London, U.K., in 1990 and 2014, respectively. From 1991 to 1994, he was a Research Scientist with the Schlumberger Cambridge Research Center, Cambridge, U.K. In 1994, he returned to Imperial College London as a Lecturer in signal processing and was promoted to Reader (Associate Professor), in 1998. From 2001 to 2004, he was the Director of the Center for Digital Signal Processing and a Professor of signal processing with the Division of Engineering, King's College London. From 2004 to 2007, he was a Cardiff Professorial Research Fellow with the School of Engineering, Cardiff University, Cardiff, U.K. From 2007 to 2014, he led the Advanced Signal Processing Group, School of Electronic, Electrical and Systems Engineering, Loughborough University, where he is currently a Visiting Professor. In 2015, he joined the School of Electrical and Electronic Engineering, Newcastle University, where he was a Professor of signal and information processing and led the ComS2IP Group and is also a Visiting Professor. In 2017, he became the Head of the School of Engineering, University of Leicester. He is also an International Honorary Dean and a Guest Professor with Harbin Engineering University, China, with support from the 1000 Talents Scheme. He is a coauthor of the books: Recurrent Neural Networks for Prediction: Learning Algorithms, Architectures and Stability (New York, NY, USA: Wiley, 2001) and EEG Signal Processing (New York, NY, USA: Wiley, 2007). He has advised more than 90 researchers through to Ph.D. graduation and published more than 500 conference papers and journal articles, many of them are in the IEEE journals. His research interests include adaptive signal processing, and machine learning and their applications. He is also a Fellow of the Royal Academy of Engineering, U.K., and the Institution of Electrical Engineers. In 2007, he received the first QinetiQ Visiting Fellowship for his outstanding contributions to adaptive signal processing and his contributions to QinetiQ, as a result of his successful industrial collaboration with the international defense systems company QinetiQ. He was the Technical Program Chair of the 15th International Conference on Digital Signal Processing and the 2009 IEEE Workshop on Statistical Signal Processing, both held at Cardiff, U.K., and a Technical Program Co-Chair of the 36th IEEE International Conference on Acoustics, Speech, and Signal Processing, Prague, Czech Republic. He has served on the IEEE Signal Processing Theory and Methods Technical Committee for six years and the IEEE Signal Processing Society Awards Board for three years, together with the Jack Kilby Award Committee. He has served as an Associate Editor for the IEEE TRANSACTIONS ON SIGNAL PROCESSING for two terms over the periods 1997–1999 and 2004–2007 and as a Senior Area Editor, from 2011 to 2014.